

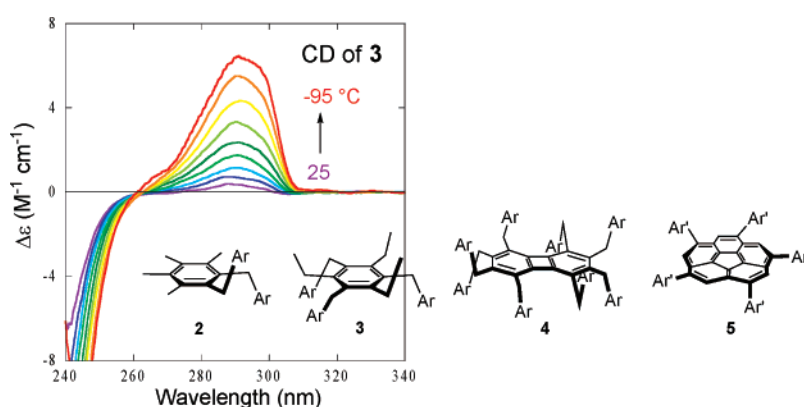
## A Combined Experimental and Theoretical Study on the Conformation of Multiarmed Chiral Aryl Ethers

Tadashi Mori,<sup>\*,†,‡</sup> Stefan Grimme,<sup>‡</sup> and Yoshihisa Inoue<sup>†</sup>

Department of Applied Chemistry, Graduate School of Engineering, Osaka University, 2-1 Yamada-oka, Suita 565-0871, Japan, and Theoretische Organische Chemie, Organisch-Chemisches Institut der Universität Münster, Corrensstrasse 40, D-48149 Münster, Germany

tiori@chem.eng.osaka-u.ac.jp

Received June 12, 2007



Four series of multiarmed chiral aryl ethers carrying two, three, five, or eight side-chains on a variety of aromatic core molecules (**2–5**) were prepared. The structure and conformation of **2** and **3** (in the solid state) were determined by the X-ray crystallographic analyses. While a pair of alternated (anti) conformers (i.e., up–down and down–up) were found in the crystal of **2**, three side-arms in **3** were aligned in the same direction to give a  $C_3$ -symmetric syn-conformation. Examinations by dispersion-corrected density functional (DFT-D) calculations revealed that two out of six anti- and two out of four syn-conformers of **2** are energetically most important. Two calculated structures of anti-conformers are in good agreement with those found in the solid state by X-ray analysis. Similarly, relevant conformations of *syn*-**3**, fully alternated **4**, and  $C_5$ -symmetric **5** were optimized at the DFT-D-B-LYP/TZVP level. The structure and conformation of the side-arms in **2–5** in solution were further studied by temperature dependent  $^1\text{H}$  NMR and UV–vis spectroscopy. In addition, comparative experimental and theoretical CD spectral studies were carried out in order to elucidate the contribution of the thermodynamically less-stable minor isomers in solution. The CD spectral changes observed for **2** and **3** at varying temperatures were quite different, while the parent chiral arene **1**, as well as **4** and **5**, only showed an increased intensity of the negative Cotton effect for the  $^1L_b$  band. The latter behavior is readily accounted for in terms of the conformational freezing of the chiral groups at low temperatures. The unusual CD spectral behavior observed for **2** and **3** was rationalized by the conformational alteration of the side-arms. Because of attractive van der Waals interactions between the aromatic units of the arms in nonpolar solvents, the syn-conformations become gradually more important for **2** at low temperatures, which eventually results in a weak positive Cotton effect for the  $^1L_b$  band. This was also supported by the SCS-MP2/TZVPP single-point energy calculations for the relevant conformers of **2**. For **3**, the contribution of the  $C_3$ -symmetrical conformer becomes more important than the less-symmetrical isomers at low temperatures. The conformations of **2** and **3** in their excited states as well as in the oxidized states were also examined.

### Introduction

Multiply substituted molecules, or molecular podands, are attracting growing interest as potential candidates for discotic

liquid crystals and hosts for organic/inorganic anions and even solvent molecules, as well as ligands for metal ions.<sup>1</sup> More recently, multiarmed compounds also have been employed as

\* To whom correspondence should be addressed. Fax: +81-6-6879-7923.

<sup>†</sup> Osaka University.

<sup>‡</sup> Universität Münster.

(1) (a) MacNicol, D. D.; Downing, G. A. *Comprehensive Supramolecular Chemistry*; Elsevier: Oxford, 1996. (b) Brunsveld, L.; Folmer, B. J. B.; Meijer, E. W.; Sijbesma, R. P. *Chem. Rev.* **2001**, *101*, 4071–4097.

a core to build dendric molecules.<sup>2</sup> These molecules possess unique features depending on the number of arms and the nature of core unit. In designing such compounds, it is essential to control the spatial arrangement of the side-arms. A number of reports have shown that the most favored arrangement in benzene derivatives is the one where all adjacent side-arms are aligned in the opposite direction to give a fully alternated conformation. For instance, X-ray crystal structures of hexakis-(4-pyridylsulfanylmethyl)benzene and octakis(2-pyridylsulfanylmethyl)biphenylene reveal that all the arms are in the anti geometry.<sup>3</sup> Such preorganization of hexasubstituted benzenes has been known for a long time.<sup>4</sup> Consequently, 1,3,5-trisubstituted triethylbenzenes have been extensively exploited as a conventional tool for aligning the arms into a  $C_3$ -symmetric syn-orientation.<sup>5</sup> Thus, a large number of successful examples of tripodal anion receptors based on this strategy have been reported,<sup>6</sup> while several other examples of such aligned tripods have employed the Kemp's triacid<sup>7</sup> and other cores.<sup>8</sup> In contrast to the tripods, control of anti/syn orientation in flexible disubstituted hosts is rather difficult.<sup>9</sup> Some recent successful reports have utilized the dipole moment of the side-arms as a means to align them in the desired orientation.<sup>10</sup>

In contrast, the binding process of guest molecules with flexible podand receptors remains more elusive.<sup>11</sup> In some cases, contrary to the preorientation strategy mentioned above, the induced fit concept becomes important for flexible hosts. For a urea-based tripodal receptor with large terminal groups, the 2-up-1-down conformer was designated as the predominant conformer by experiments and theory.<sup>12</sup> The <sup>1</sup>H NMR study of the Enterobactin-analogues also showed the possible rotation of the

side-arms.<sup>13</sup> In fact, such exceptions have been reported occasionally and also found in the crystal structures.<sup>14,15</sup> For some dipods, the syn-form is readily induced upon (electro)-chemical oxidation, as demonstrated by X-ray crystallographic analysis of the resulting radical cation.<sup>16</sup> Such conformational changes associated with the  $\pi$ -stacking of radical cation were also reported for other systems.<sup>17</sup> Accordingly, although the (fully) alternated form is energetically most favored in most of the cases, other (partially alternated or partially syn) conformations should also be considered, especially in solution in order to understand the binding behavior in detail. It is also expected that slight environmental changes, for example in temperature or solvent polarity, should affect the population of the conformers. Such conformational interconversion has, however, been investigated only recently for 3-aminopyridinium-based tripodal hosts.<sup>18</sup> Therefore, our goal is to track the static and dynamic behaviors of side-arm conformations in multiarmed compounds through the investigation of their experimental and theoretical chiroptical properties.

In this study, we synthesized new chiral multiarmed compounds (**2–5**) and examined and discussed the spectroscopic changes associated with the possible conformation(s) and dynamics of the side-arms in detail, focusing on the experimental and theoretical circular dichroism (CD)<sup>19</sup> spectra. Scheme 1 summarizes the possible conformational changes of the relevant polytentacled aryl ethers **2–5**. We have chosen the aromatic pendants with simple chiral (*R*)-2-methylpropyloxy group(s) to observe the chiroptical signals required for the present study (A). Obviously, the fundamental conformational variation is based on the relative up–down/down–down (or anti/syn) orientation of the side-arms. In addition to such anti/syn conformation, up–down and down–up conformers should be separately considered (in the case of chiral dipod **2**), because they are in diastereomeric relationship due to the chirality in the side-arm (B). Note that these two conformers are essentially mirror-imaged in structure, if one ignores the chiral group in the side-arm. In some cases upon incorporating unsymmetrically substituted side-arms, there is an additional pair of conformers originating from the orientation of the aromatic plane of the side-arm (see A in Scheme 1). To sum up, six up–down and four down–down skeletal conformers are possible, and all of them were considered in the following study. For simplicity, the conformation of the terminal alkyl group was ignored throughout this study (*vide infra*). For tripod **3** and octapod **4**, all possible fully alternated conformers were considered (C and D). A possible involvement of the partially alternated conformers (which contain one syn or down–down orientation) was also considered briefly. In the case of corannulene-based **5**, side-

(2) Newkome, G. R.; Moorefield, C. N. *Densritic Molecules: Concepts, Syntheses, Perspectives*; VCH: New York, 1996.

(3) McMorran, D. A.; Steel, P. J. *Tetrahedron*, **2003**, *59*, 3701–3707.

(4) MacNicol, D. D.; Hardy, A. D. U.; Wilson, D. R. *Nature* **1977**, *266*, 611–612.

(5) For reviews on the unique features of 1,3,5-trisubstituted triethylbenzenes in host-guest chemistry, see: Hennrich, G.; Anslyn, E. V. *Chem. Eur. J.* **2002**, *8*, 2219–2224. (b) Best, M. D.; Tobey, S. L.; Anslyn, E. V. *Coord. Chem. Rev.* **2003**, *240*, 3–15. (c) Wiskur, S. L.; Ait-Haddou, H.; Lavigne, J. J.; Anslyn, E. V. *Acc. Chem. Res.* **2001**, *34*, 963–972.

(6) (a) Frontera, A.; Morey, J.; Oliver, A.; Pina, M. N.; Quinero, D.; Costa, A.; Ballester, P.; Deya, P. M.; Anslyn, E. V. *J. Org. Chem.* **2006**, *71*, 7185–7195. (b) Wright, A. T.; Griffin, M. J.; Zhong, Z.; McCleskey, S. C.; Anslyn, E. V.; McDevitt, J. T. *Angew. Chem., Int. Ed.* **2005**, *44*, 6375–6378. (c) Wiskur, S. L.; Floriano, P. N.; Anslyn, E. V.; McDevitt, J. T. *Angew. Chem., Int. Ed.* **2003**, *42*, 2070–2072. (d) Zhong, Z.; Anslyn, E. V. *J. Am. Chem. Soc.* **2002**, *124*, 9014–9015. (e) Metzger, A.; Anslyn, E. V. *Angew. Chem., Int. Ed.* **1998**, *37*, 649–652. (f) Metzger, A.; Lynch, V. M.; Anslyn, E. V. *Angew. Chem., Int. Ed.* **1997**, *36*, 862–865.

(7) (a) Kemp, D. S.; Petrakis, K. S. *J. Org. Chem.* **1981**, *46*, 5140–5143. See, also: (b) Bauerl, A.; Westkämperl, F.; Grimme, S.; Bach, T. *Nature*, **2005**, *436*, 1139–1140. (c) Bach, T.; Bergmann, H.; Grosch, B.; Harms, K. *J. Am. Chem. Soc.* **2002**, *124*, 7982–7990.

(8) (a) Fabris, F.; Pellizzaro, L.; Zonta, C.; De Lucchi, O. *Eur. J. Org. Chem.* **2007**, 283–291. (b) Abe, H.; Aoyagi, Y.; Inouye, M. *Org. Lett.* **2005**, *7*, 59–61.

(9) (a) Singh, P.; Kumar, S. *Tetrahedron*, **2006**, *62*, 6379–6387. (b) McMorran, D. A.; Hartshorn, C. M.; Steel, P. J. *Polyhedron*, **2004**, *23*, 1055–1061. (c) McMorran, D. A.; Steel, P. J. *Inorg. Chem. Commun.* **2003**, *6*, 43–47. (d) Kilway, K. V.; Siegel, J. S. *Tetrahedron* **2001**, *57*, 3615–3627.

(10) (a) Cort, A. D.; Gasparrini, F.; Lunazzi, L.; Mandolini, L.; Mazzanti, A.; Pasquini, C.; Peirini, M.; Rompietti, R.; Schiaffino, L. *J. Org. Chem.* **2005**, *70*, 8877–8883. (b) Betson, M. S.; Clayden, J.; Lam, H. K.; Helliwell, M. *Angew. Chem., Int. Ed.* **2005**, *44*, 1241–1244.

(11) Steed, J. W.; Atwood, J. L. *Supramolecular Chemistry*; John and Wiley & Sons: Chichester, 2000.

(12) Turner, D. R.; Paterson, M. J.; Steed, J. W. *J. Org. Chem.* **2006**, *71*, 1598–1608.

(13) Stack, T. D. P.; Hou, Z.; Raymond, K. N. *J. Am. Chem. Soc.* **1993**, *115*, 6466–6467.

(14) Menger, F. M.; Azov, V. A. *J. Am. Chem. Soc.* **2002**, *124*, 11159–11166.

(15) Taha, M.; Marks, V.; Gottlieb, H. E.; Biali, S. E. *J. Org. Chem.* **2000**, *65*, 8621–8628.

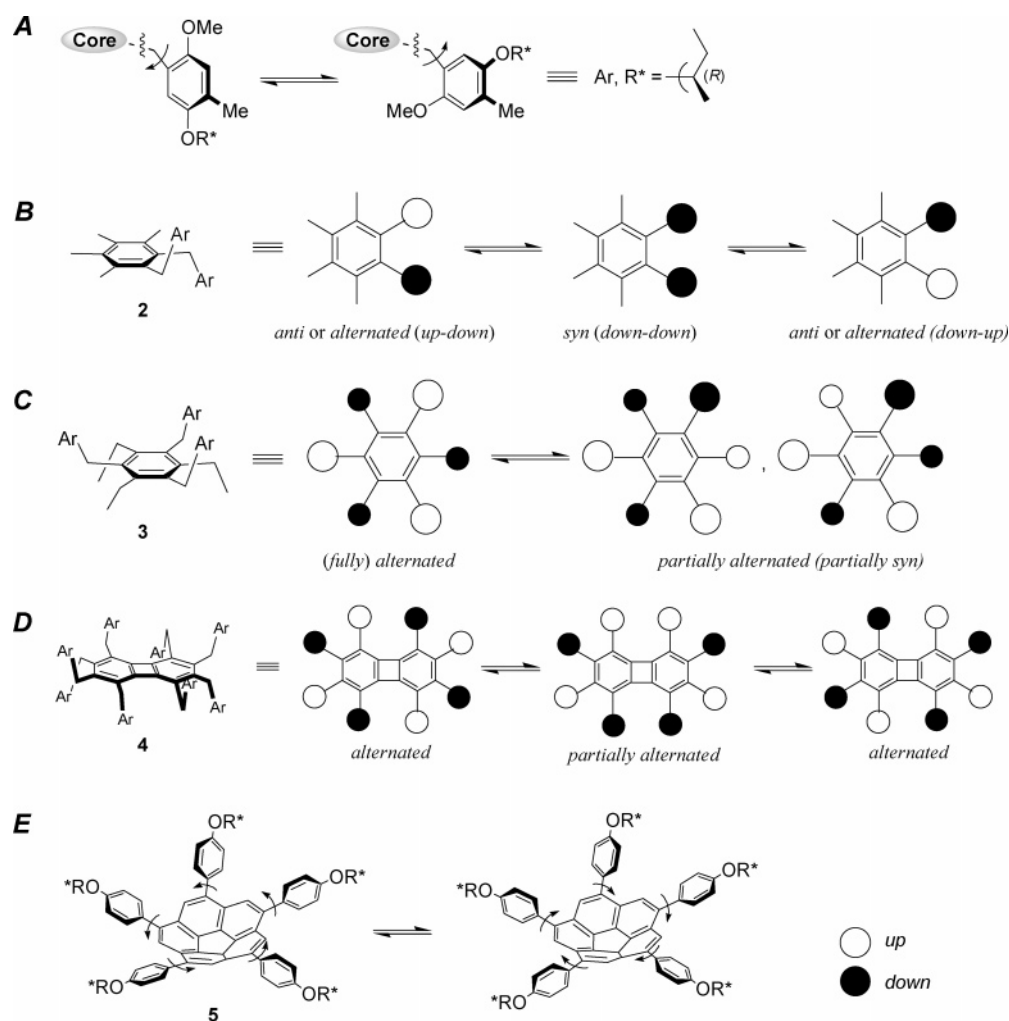
(16) Sun, D. L.; Rosokha, S. V.; Lindeman, S. V.; Kochi, J. K. *J. Am. Chem. Soc.* **2003**, *125*, 15950–15963.

(17) (a) Rathore, R.; Chebny, V. J.; Kopatz, E. J.; Guzei, I. A. *Angew. Chem., Int. Ed.* **2005**, *44*, 2771–2774. (b) Rathore, R.; Chebny, V. J.; Abdelwahed, S. H. *J. Am. Chem. Soc.* **2005**, *127*, 8012–8013.

(18) Wallace, K. J.; Belcher, W. J.; Turner, D. R.; Syed, K. F.; Reed, J. W. *J. Am. Chem. Soc.* **2003**, *125*, 9699–9715.

(19) (a) Berova, N.; Nakanishi, K.; Woody, R. W. *Circular Dichroism, Principles and Applications*, 2nd ed.; John Wiley & Sons: New York, 2000. (b) Lightner, D. A.; Gurst, J. E. *Organic Conformational Analysis and Stereochemistry from Circular Dichroism Spectroscopy*; John Wiley & Sons: New York, 2000.

SCHEME 1. Conformational Variations of 2–5



arms are attached directly to the scaffold. Thus, two possible  $C_5$ -symmetrical conformations, where the side-arms are tilted to the opposite direction, were considered (E). These conformers interconvert either by synchronized aryl–aryl bond rotations or by concave–convex inversion of the corannulene moiety. Several other combinations of partially syn (alternated) conformers were also possible, but we only address the simple  $C_5$  conformations in this study.

## Results and Discussion

**Structural Studies of Multi-armed Chiral Aryl Ethers. (a) X-ray Crystallographic Studies of 2 and 3.** The single crystals suitable for X-ray crystallographic analyses were obtained by slow evaporation of the ethanol solutions of **2** or **3**, containing diethyl ether or dichloromethane, respectively. All the data collections were performed at  $-60\text{ }^\circ\text{C}$ , since the chiral (1-methylpropyl) group tends to disorder at ambient temperatures according to our previous experiences. This clearly indicates that the conformation of the chiral group(s) is not completely fixed at a single orientation in both solid and condensed phases, especially at elevated temperatures. Nevertheless, the final residues of the refinement on both structures at this temperature were fairly good ( $R = 7.4$  and  $7.6\%$  for **2** and **3**, respectively). The PLUTO drawings, thus obtained for **2** and **3**, are shown in Figure 1. More details of the X-ray structural determination as

well as ORTEP drawings and crystal packing diagrams are found in Supporting Information.

The crystalline **2** bears two independent molecules in the unit cell, which can be ascribed to the chirality in the portal group. Both of these molecules are in an anti orientation with respect to the chiral arms, thus possessing  $C_2$  symmetry. Accordingly, two conformers, i.e., up–down and down–up, are found in crystals and they are alternately aligned in the crystalline lattice. Although they are diastereomers, the dihedral angles between the core and side-arm aromatic planes are almost identical:  $99.7^\circ \pm 0.2^\circ$  (Table S-1 in Supporting Information). The anti orientation of **2** in the solid state is in accord with the reported crystallographic structure of an achiral analogue, 1,2-bis(2,5-dimethoxy-4-methyltolyl)tetramethylbenzene.<sup>16</sup>

The structure determination of **3** revealed that there are also two independent molecules in the unit cell. Both of these enjoy fully alternated up–down disposition with respect to the side-arms, adopting quasi- $C_3$  symmetry. Consequently, the chiral donor moieties are aligned in an all-syn orientation to the central ring. This is in accord with the reported X-ray structures of hexaethylbenzene ( $D_{3h}$ )<sup>20</sup> and 1,3,5-tris(*p*-methoxybenzyl)triethylbenzene ( $C_3$ ).<sup>21</sup> More importantly, three peripheral rings

(20) Iverson, D. J.; Hunter, G.; Blount, J. F.; Damewood, J. R., Jr.; Mislow, K. *J. Am. Chem. Soc.* **1981**, *103*, 6073–6083.

(21) Simaan, S.; Siegel, J. S.; Biali, S. E. *J. Org. Chem.* **2003**, *68*, 3699–1701.

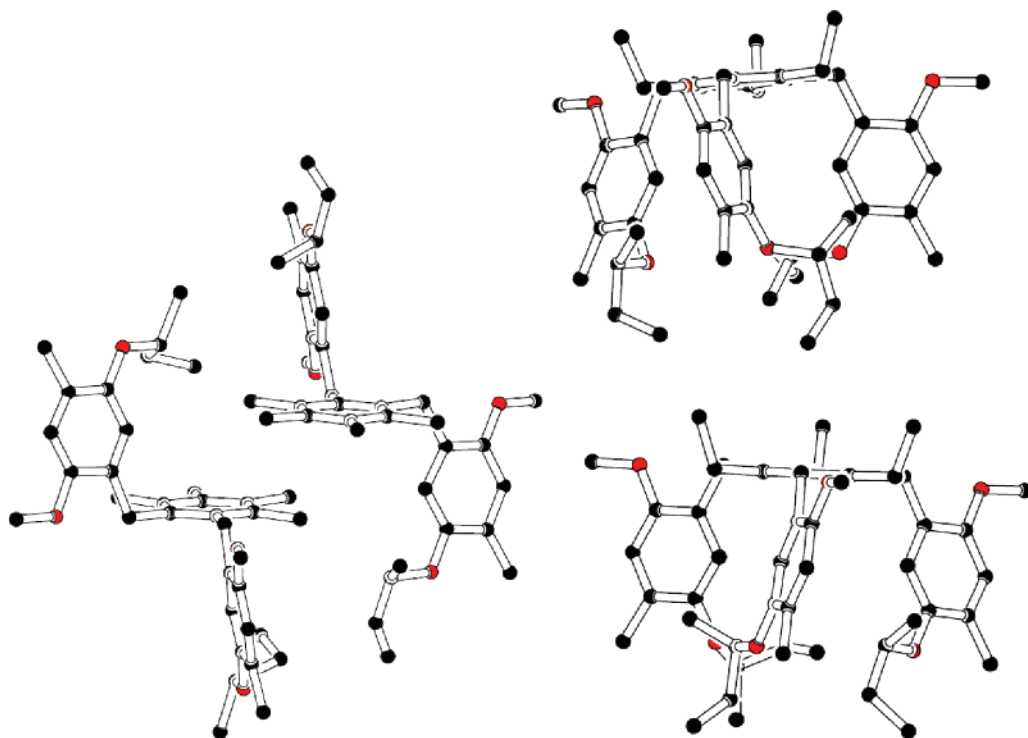


**FIGURE 1.** X-ray structures of **2** and **3** (PLUTO drawings). Pairs of independent structures were found for both **2** (left) and **3** (right) in the each unit cell. They are diastereomeric to each other with the up–down vs down–up conformations in **2**, while they differ only in tilt angles in **3**.

in the latter compound are oriented in the H-perpendicular arrangement.<sup>21</sup> The two conformers in the crystal of **3** differ structurally in tilt angles. Thus, their side-arms are tilted in the opposite direction, but all are in the H-perpendicular arrangement. A close inspection of the structure revealed that the tilt angles of these perpendicularly arranged arms are entirely different among the three moieties for both conformers, where one of these arms is essentially situated in the almost eclipsed arrangement. Unfortunately, no single crystals suitable for the X-ray structural analysis were obtained for **4** and **5**, despite our repeated attempts under a variety of conditions.

**(b) Geometrical Optimization of Multi-armed Chiral Aryl Ethers 2–5 by Density Functional Theory.** The geometries of a variety of conformers of polytentacled donors **2–5** were investigated using the DFT-D-B-LYP method. The DFT-D method exploits an empirical correction by adding pairwise  $-C_6/R^6$  potentials to describe van der Waals (vdW) interactions. The method is computationally as efficient as conventional DFT calculations, and the calculated energies and geometries are fairly comparable to those obtained with the improved SCS-MP2 method.<sup>22</sup> Thus, DFT-D is a very efficient practical alternative for large molecules where the more accurate electron correlated methods such as (SCS)-MP2 or CCSD(T) cannot be applied. A number of successful applications of the DFT-D method have been reported recently, e.g., for weakly bonded intermolecular complexes<sup>23</sup> and relatively large host–guest

molecules<sup>24</sup> (for an overview, see ref 25). Here, we first examined the validity of the DFT-D geometry optimization applied to the present systems to reveal that the X-ray structures of **2** and **3** are accurately reproduced by the calculations, despite the apparent difference in “phase” (solid versus gas). Accordingly, we employed this approach to optimize various conformers of **2** and **3**, and further extended the theoretical treatment to the much larger systems (**4** and **5**) as follows.

**1,2-Bis(arylmethyl)-3,4,5,6-tetramethylbenzene 2.** All of the conformations of **2** were fully optimized at the DFT-D-B-LYP/TZVP level. As briefly described in the Introduction, the up–down and the down–up conformers were separately considered because they become different by introducing chirality in the side-arms (Scheme 1). They are expected to give completely different (and most probably almost mirror-imaged) CD profile because of their diastereomeric structure, in which the relative structures of aromatic rings are in enantiomeric relationship. In addition, since the substituent on the benzene ring of the arm is not symmetrical, there are additional pairs with respect to the orientation of the aromatic plane. Thus, there are six up–down and four down–down skeletal conformers in total. Note that the conformation of the chiral group was taken always as the  $Tg^-$  conformation throughout this study.<sup>26</sup> Among all the optimized structures, two up–down (**2a**, **2b**) and two down–down (**2g**, **2h**) conformations were found to be energetically feasible (population  $\geq 5\%$ ). The optimized structures of these four conformers are shown in Figure 2, and details of the

(22) (a) Grimme, S. *J. Phys. Chem. A* **2005**, *109*, 3067–3077. (b) Goumans, T. P. M.; Ehlers, A. W.; Lammertsma, K.; Würthwein, E.-U.; Grimme, S. *Chem. Eur. J.* **2004**, *10*, 6468–6475. (c) Grimme, S. *J. Chem. Phys.* **2003**, *118*, 9095–9102. (d) Gerenkamp, M.; Grimme, S. *Chem. Phys. Lett.* **2004**, *392*, 229–235. (e) Grimme, S. *J. Comput. Chem.* **2003**, *24*, 1529–1537. (f) Piacenza, M.; Grimme, S. *J. Comput. Chem.* **2004**, *25*, 83–99.

(23) (a) Grimme, S.; Diedrich, C.; Korth, M. *Angew. Chem., Int. Ed.* **2006**, *45*, 625–629. (b) Piacenza, M.; Grimme, S. *J. Am. Chem. Soc.* **2005**, *127*, 14841–14848 (c) Piacenza, M.; Grimme, S. *Chem. Phys. Chem.* **2005**, *6*, 1554–1558.

(24) Parac, M.; Etinski, M.; Peric, M.; Grimme, S. *J. Chem. Theory Comput.* **2005**, *1*, 1110–1118.

(25) Grimme, S.; Antony, J.; Schwabe, T.; Mück-Lichtenfeld, C. *Org. Biomol. Chem.* **2007**, *7*, 741–758.

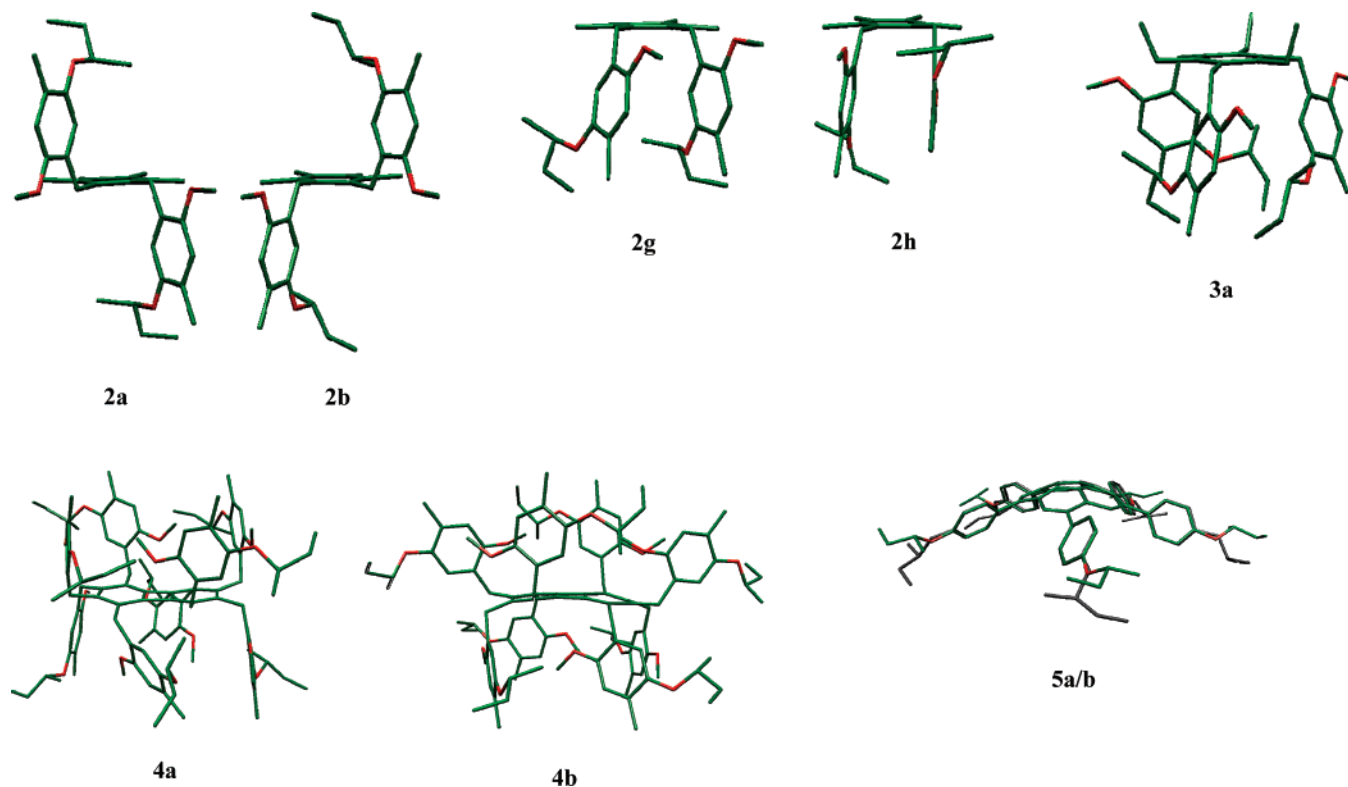


FIGURE 2. The DFT-D-B-LYP/TZVP optimized structures of most stable conformers of multiarmed chiral aryl ethers 2–5.

calculation are summarized in Table 1 (see Supporting Information for all the optimized geometries). The structures of two up–down conformers (**2a**, **2b**) obtained by the DFT-D method show reasonable agreement with those obtained by the X-ray structural analyses. Although two types of conformation were found in (complete) 1:1 ratio in the crystals, the energy difference calculated by the SCS-MP2 method indicates that the up–down conformer **2a** is slightly preferred by  $\sim 0.1$  kcal mol $^{-1}$  over the diastereomeric **2b**. Indeed, this slight preference turned out to be very important in understanding the experimental CD spectra (*vide infra*). A similar situation has already been reported for the axial chirality in biaryls,<sup>26</sup> where most of the CD signals are canceled out between the conformers of almost opposite chirality, but still the remnants sum up to give a small but appreciable Cotton effect in the CD spectra. Two down–down (**2g**, **2h**) conformers were also considered since these conformers should be involved in the interconversion process of the side-arms. The overall calculated preference for the down–down conformers over the up–down/down–up conformers in the gas phase is ascribed mostly to the large vdW attraction between the substituents for which the dispersion term is responsible. Note that our calculations completely ignore the solvent effect, and therefore the relative energies of the down–down conformers are intrinsically underestimated.

**1,3,5-Tris(arylmethyl)-2,4,6-triethylbenzene 3.** The geometry optimization of **3** was also performed at the DFT-D-B-LYP/TZVP level employing  $C_3$  symmetry (i.e., fully alternated form, Scheme 1). In our calculation, only one conformation (**3a**) was found to be feasible (Figure 2), and the optimized structure is in excellent agreement with one of the two structures found in the crystal. Another conformer, in which the side-arms are tilted to the opposite direction, did not give a local minimum upon calculations. The latter conformer found in the crystal is, therefore, considered to be stabilized by the packing forces in

the crystal. Two additional conformers (**3b**, **3c**), which arise from the different orientation of the side-arm, were optimized by the calculations. These conformers, however, possess larger steric repulsion between the methoxy groups and are thus higher in energy by more than  $\sim 15$  kcal mol $^{-1}$  (Table S-2 in Supporting Information). Therefore, such conformers are practically nonexistent in solution. Similarly, other conformers with one or two flipped side-arm(s) (partially alternated conformers, Scheme 1) were not considered because they are also expected to have higher relative energies. In the following, only the most stable conformer **3a** is considered in further simulations of the CD spectra of **3**.

**Octakis(arylmethyl)biphenylene 4.** Geometry optimization of a molecule of this size (132 non-hydrogen and 152 hydrogen atoms) by quantum chemical methods is challenging, even when the very efficient DFT-D method is applied. By using a parallel computing system and the resolution of identity approximation<sup>47</sup> (RI) and employing  $C_2$ -symmetry, we have successfully optimized two fully alternated conformations of **4** at the DFT-D-B-LYP/TZVP level within reasonable computation times. The two calculated conformers (**4a**, **4b**) were in a diastereomeric relationship; the side-arms are in an alternated form and aligned either up–down–up or down–up–down manner (Figure 2). The relative energies at the DFT-D level were found to be quite similar ( $\Delta E \sim 0.3$  kcal mol $^{-1}$ ) between **4a** and **4b** despite having eight arms. The SCS-MP2/TZVPP energy calculations were not possible because of the size of molecule (Table S-2). The partially syn (alternated) conformations (Scheme 1) found in the crystal structure of octaethylbiphenylene<sup>15</sup> were not feasible in the present molecule because of the large steric hindrance of the side-arms and therefore not considered further.

**Pentaarylcorannulene 5.** The geometrical optimization of **5** was also performed at the same level employing the  $C_5$  symmetry restrictions. Two conformations, in which the relative

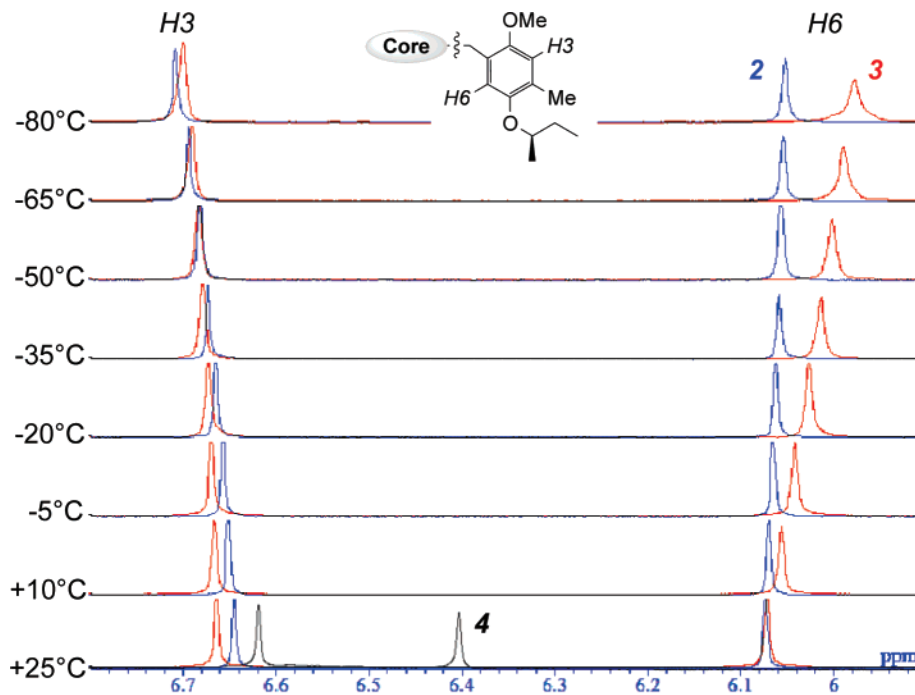


**FIGURE 3.** Temperature dependence of the  $^1\text{H}$  NMR spectra of **2** and **3** (and **4** at 25 °C) in dichloromethane- $d_2$ . For other regions, see Figure S-8 in Supporting Information.

orientations of the alkoxy group are inverted, were obtained as the most stable structures. Both structures (**5a**, **5b**) are displayed in Figure 2, which demonstrates that the relative orientations of the aromatic rings in the side-arms are almost identical. However, one of the conformers (**5a**) is slightly favored by  $\sim 0.2$  kcal mol $^{-1}$ , as determined by the SCS-MP2/TZVPP energy calculations. The other conformers, in which the aromatic planes of the side-arms are tilted to the opposite direction, were found much less stable (by  $\sim 7$  kcal mol $^{-1}$ ). Therefore, they will not affect the overall spectra and are not considered further.

**Variable Temperature  $^1\text{H}$  NMR Studies of **2** and **3**.** To experimentally gain information on the conformational changes of **2** and **3** in solution, we performed  $^1\text{H}$  NMR spectral studies at varying temperatures in dichloromethane- $d_2$  (Figure 3). As the temperature of the solution was decreased, the aliphatic protons of the chiral group of **2** and **3** became broad and structureless, e.g., at  $-80$  °C (Figure S-8 in Supporting Information). This implies that the peripheral alkyl group(s) are gradually fixed at lower temperatures and the rotation of the alkyl group(s) becomes slow in the NMR time-scale. The changes of chemical shift in the aromatic protons, as a measure of the side-arm dynamics, are compared in Figure 3. The H6 proton adjacent to the chiral alkoxy group (and thus most crowded) is highly shielded in **2** and **3** compared with that in **4** (and **1**, see Supporting Information for the details). As determined by X-ray structural analyses and also by the DFT-D calculations, this proton is located just above (or below) the central aromatic ring (see Figures 1 and 2). By lowering the temperature, the H6 was further shielded gradually, and this tendency was much pronounced for **3**. The H6 in **3** appeared as a broad peak at a chemical shift as low as  $\sim 6$  ppm at  $-80$  °C. This is rationalized by assuming that the side-arms are more closely located to each other on the same side of the aromatic core in **3** at lower temperatures to make the H6 protons overcrowded and affected more severely by the neighboring

protons. The opposite tendency observed for the H3 proton (para to H6) can be similarly explained. Thus, the deshielding effect observed for the outside H3 of **2** at lower temperatures is quite reasonable, as the inside H6 is shielded by the ring current of the benzene core. The effect of deshielding was smaller for **3**, probably because the steric repulsion between the inside H6 protons, all of which are facing the center of the aromatic ring, prevents more tight packing. Therefore, the H3 protons in **3** are anticipated to be slightly deviated from the center of the ring (as compared with **2**), and the effect of ring current is attenuated.

In the above NMR experiments, a gradual freezing of the side-arms upon cooling was confirmed for **2** and **3**. This is commonly observed behavior, but does not tell about the possibility of the side-arm rotation to form the partially alternated conformers. In the following, we investigated the effect of temperature on the circular dichroism (CD) of **2–5**. By analyzing the experimental and theoretical CD spectra, we were able to detect the possible rotation of the arm(s) leading to the partially alternated conformations.

**Measurement of UV-vis and CD Spectra of Multiarmed Chiral Aryl Ethers **2–5**. (a) Experimental CD Spectra of **2** and **3**.** The CD spectra of **2** were obtained in dichloromethane solution at temperatures between 25 and  $-95$  °C (Figure 4, top, left). The corresponding UV-vis spectra as well as the anisotropy ( $g$ ) factors ( $g = \Delta\epsilon/\epsilon$ ), both observed with the same solutions, are also shown in Figure S-9 in Supporting Information. The CD spectrum of **2** at 25 °C shows negative and positive Cotton effects at the  $^1\text{L}_b$  (290 nm) and the  $^1\text{L}_a$  (230 nm) bands, respectively. This pattern is quite similar to the CD spectrum of the parent chiral benzene **1** (Figure S-13 in Supporting Information). A slightly smaller molar ellipticity observed for **2** (having two chiral auxiliaries) is probably due to a cancellation of the oppositely signed Cotton effects of the relevant (diastereomeric) conformers. Upon cooling, a positive Cotton effect

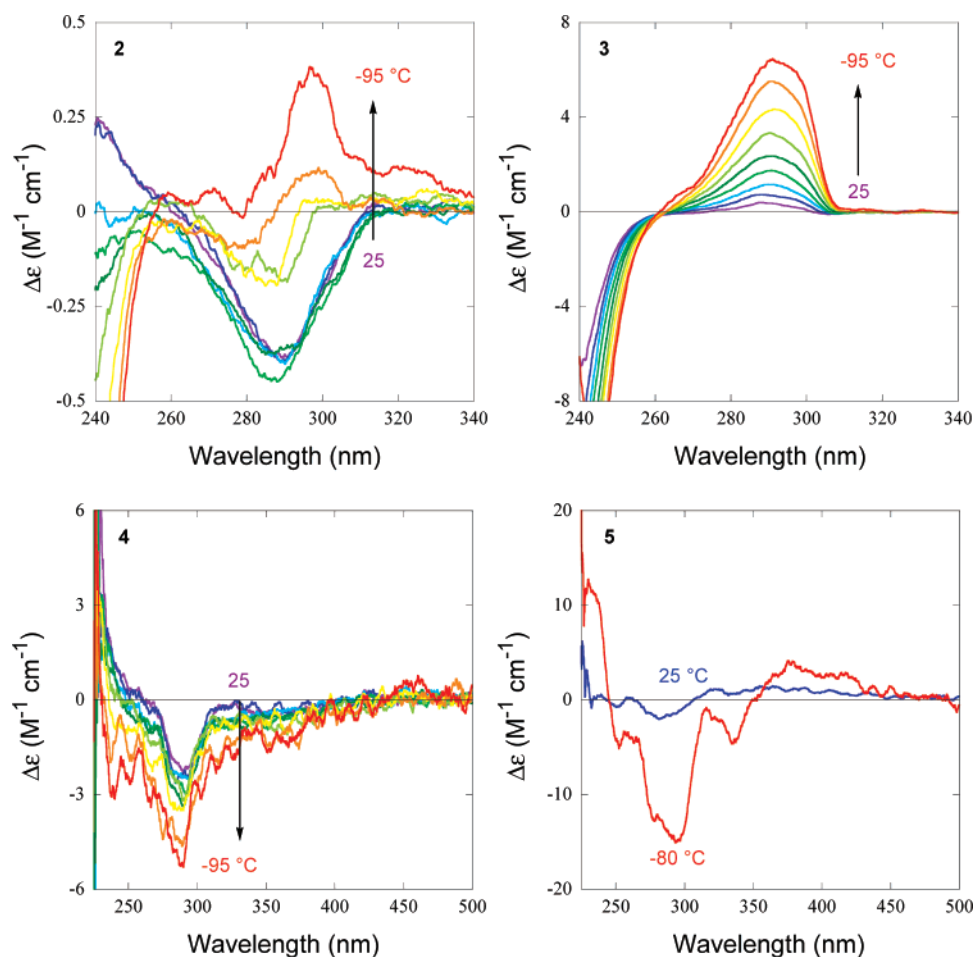


**FIGURE 4.** Temperature dependence of the CD spectra of **2–4** (and **5** at 25 and  $-80$  °C) in dichloromethane at temperatures varied from 25 to  $-95$  °C at an interval of 15 °C.

peak appeared at slightly longer wavelengths in the  $^1L_b$  transition region (300 nm). Thus, apparently bisignate CD spectra were obtained in this  $^1L_b$  region at temperatures between  $-50$  and  $-80$  °C. At  $-95$  °C, a positive Cotton effect was observed at  $^1L_b$  band (300 nm), together with a negative Cotton effect at the  $^1L_b$  band (240 nm).

This temperature effect on the CD spectra of **2** is puzzling but may be rationalized by assuming a larger contribution of the partially alternated conformation(s) at lower temperatures as follows. A comparison of the temperature effects on the CD spectra of **2** and **1** (Figure 4 and Figure S13) led us to a conclusion that the typical CD spectral changes observed for **2** should not be attributed to the side-arm conformation alone but to the arm–arm and/or arm–core orientations. The fact that the CD spectrum of **2** is almost identical to that of **1** at 25 °C implies that the CD signals arising from the arm–arm and/or arm–core orientations are almost canceled out at least at ambient temperatures. Considering the fact that the all-syn conformer of **3** affords a strong positive Cotton effect (*vide infra*), we may deduce that the partially alternated (i.e., syn or down–down) conformer(s) becomes more important, leading to the sign inversion of the CD spectra of **2**, at low temperatures. Nevertheless, as the CD intensity of **2** is always weak relative to that of **3**, contribution of the partially alternated conformers is modest even at the lower temperatures.

The temperature dependence behavior of the UV–vis spectra of **3** was quite similar to that of **2** (Figure S-10 in Supporting

Information). By lowering the temperature, a small blue shift of the  $^1L_b$  band maximum was observed for both **2** and **3**. In contrast, the temperature effect on the CD spectrum of **3** was considerably different from that of **2**. As shown in Figure 4 (top, right), positive and negative Cotton effects observed for the  $^1L_b$  (290 nm) and  $^1L_a$  (230 nm) bands of **3** steadily became stronger as the temperature was decreased. The CD intensities of the  $^1L_b$  and the  $^1L_a$  bands are 20 times larger for **3** than for **2** at  $-95$  °C. As was indicated by the VT-NMR studies (*vide supra*), the three side-arms in **3** are basically aligned in the same direction, which gradually packed tightly as the temperature decreases. However, it is quite rational to consider that the conformational alteration of side-arms is also involved in **3**, especially at higher temperatures. Lowering temperature reduces the contribution of such partially alternated conformers of **3** in solution. These explanations are consistent with the results that simple freezing of the chiral group in **1** only slightly enhances (by a factor of 2) the CD intensity (Figure S-13 in Supporting Information), but **2** and **3** display the totally different CD spectral behavior (intensity change).

**(b) Comparison of Solvent Effects on the CD Spectra of **2** and **3**.** The effect of solvent on the CD spectra of **2** and **3** provides additional insights into the dynamic behavior of the side-arms of the molecules. For **2**, the above-mentioned temperature effect was only observed in less polar solvents such as methylcyclohexane and dichloromethane. Interestingly, the effect of the temperature was less significant in more polar

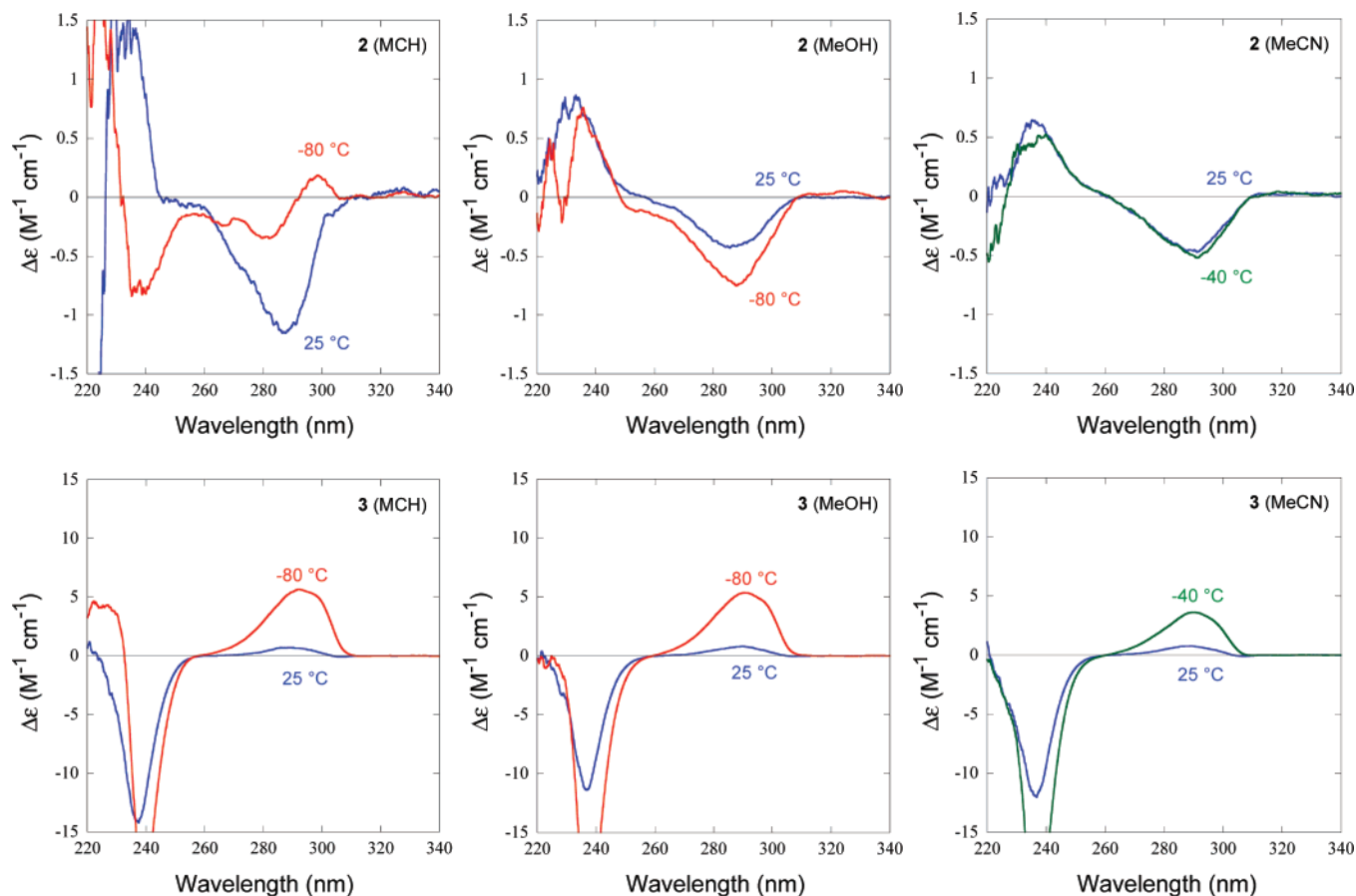


**FIGURE 5.** CD spectra of **2** (top) and **3** (bottom) in methylcyclohexane (left), methanol (middle), and acetonitrile (right) at two different temperatures (0.1 mM).

methanol and acetonitrile (Figure 5, top), which is quite similar to that found for **1**. Thus, the arm–arm and/or arm–core CDs are almost canceled out in the observed spectrum of **2** in polar solvents at any temperatures examined, and what we observed in the VT–CD spectra of **2** in polar solvents is a consequence of simple freezing of the chiral auxiliaries. In less polar solvents at low temperatures, the partially alternated (down–down) conformers become apparent, probably because of the pronounced  $\pi$ – $\pi$  (dispersion) interaction between the arms. Such intramolecular interactions are not feasible in polar solvents because of the more preferred solvation.

In sharp contrast to **2**, **3** exhibited a more straightforward temperature effect in all the solvents examined, giving an increased CD intensity at a reduced temperature (Figure 5, bottom). The simplest explanation for this CD spectral behavior of **3** is that the syn- $(C_3)$ -conformer becomes dominant at low temperatures in all solvents. Accordingly, the CD intensities increase with decreasing population to the partially alternated conformers, which are pseudo-centrosymmetric, and thus the CD signals are mutually canceled between the oppositely oriented side-arms to give weaker Cotton effects.

**(c) CD Spectra of 4 and 5.** The CD spectra of **4** in dichloromethane at temperatures ranging from 25 to  $-95$  °C were also obtained and are shown in Figure 4 (bottom, left). As the temperature decreases, the negative Cotton effect at the  $^1L_b$  band (290 nm) gradually increases. The (induced) Cotton effect at around 300 nm is not apparent at any temperature in the wavelength range corresponding to the absorption of the biphenylene core (see also Figure S-11 in Supporting Informa-

tion). The molar circular dichroism ( $\Delta\epsilon$ ) of the negative Cotton effect at the  $^1L_b$  band of **4** was roughly 8 times larger than that of **1**. Since the adjacent bromomethyl groups (instead of arylmethyl groups in this study) in polysubstituted arenes are already conformationally fixed at room temperature (on the NMR time-scale),<sup>26</sup> the much larger side-arms in **4** are completely fixed in the fully alternated form at temperatures lower than 25 °C. Thus, the above-mentioned spectral change can be explained by a conformational freezing of the chiral auxiliaries by lowering the temperature. Thus, the temperature effects in different solvents (methylcyclohexane and methanol) are very similar to that in dichloromethane (Figure S-14 in Supporting Information).

The UV–vis and CD spectra of **5** were also measured in dichloromethane at 25 and  $-80$  °C (Figure 4, bottom, right, and Figure S-12 in Supporting Information). The (induced) Cotton effects of **5** at around 300 nm were not apparent at the absorption bands corresponding to the corannulene core, as was similarly observed for the spectral changes of **4**. At a low temperature, the negative Cotton effect corresponding to the  $^1L_b$  band of the side-arms became larger. Considering the free rotation of the side-arms as well as rapid bowl inversion of the

(26) The effect of the minor conformers in respect to the terminal alkyl group as well as overall simulated UV/CD spectra therefrom is considered to be very small according to our previous experience. For a detailed discussion of the effect of the conformation of the terminal chiral group, see: Mori, T.; Inoue, Y.; Grimme, S. *J. Phys. Chem. A* **2007**, *111*, 4222–4234.



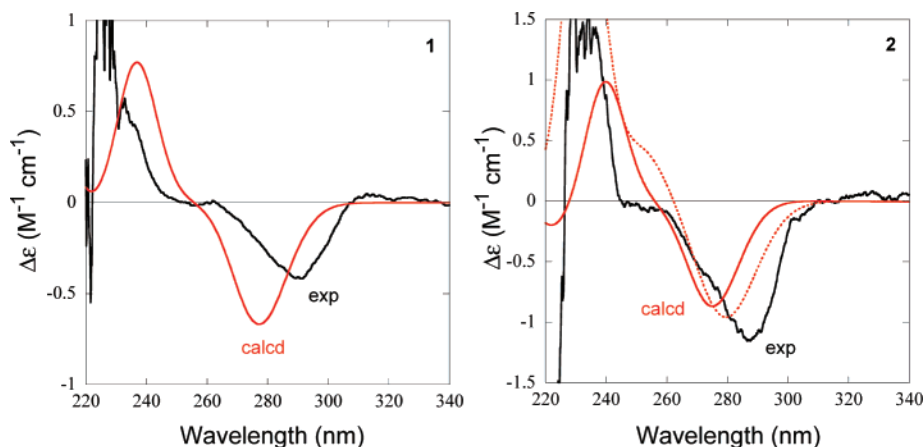


**FIGURE 6.** Comparison of the experimental and calculated CD spectra of **1** (left) and **2** (right). Black: experimental CD spectra in dichloromethane at 25 °C. Red: TD-DFT-BH-LYP/TZVP calculated CD spectra. For **2**, solid line: calculated spectrum averaged over all up–down conformers (**2a–f**); dotted line: calculated spectrum averaged over all possible conformers (**2a–j**).

corannulene core in **5**,<sup>27,28</sup> this temperature effect can be ascribed to a freezing of the chiral auxiliaries at the low temperature.

**(d) Theoretical Calculation of the CD Spectrum of 2.** The TD-DFT based computation of rotatory strengths and CD spectra has been successfully applied recently to the assignment of the absolute configuration and conformation of chiral organic molecules.<sup>29,30</sup> Accordingly, we performed TD-DFT calculations for all 10 conformers of **2** at the BH-LYP/TZVP level to simulate the UV–vis and CD spectra. The choice of the functional and the basis-sets is based on previous experience.<sup>26,31</sup> The validity of our method was confirmed by the successful reproduction of the experimental CD spectrum of **1** by theoretical calculations (Figure 6, left). While the computed UV–vis spectra of all possible conformers of **2** are essentially the same, the CD spectra are considerably different from each other. The theoretical CD spectrum of **2**, shown in Figure 6 (right), was obtained as a Boltzmann population-weighted average of the CD spectra of all conformers based on their SCS-MP2 relative energies. Such a static approach<sup>32</sup> nicely reproduced the pattern and relative rotatory strength of the experimental CD spectra of **2**. The first negative and the second positive Cotton effects were correctly predicted, although a slightly larger scaling factor

(1/20) was necessary to fit to the experimental values. Since the dynamic equilibrium between up–down and down–up conformers becomes evident, we further tested the effect of partially alternated conformers (i.e., syn or down–down conformers). The experimental spectrum is only slightly better reproduced when the contributions of the partially alternated conformations are considered (Figure 6, right), but we were not able to estimate the magnitude of contribution from such conformers.

Theoretical computations of the CD spectra of **3–5** were also conducted by the same TD-DFT method as well as by a semiempirical  $\pi$ -electron time-dependent Pariser–Parr–Pople (TD-PPP) scheme.<sup>33</sup> The calculations of UV–vis and CD spectra were performed for energetically relevant conformers of **3–5** (i.e., **3a**, **4a**, **4b**, **5a**, and **5b**). The computation of the CD spectrum of **4** was only possible with DFT-D energy-based averaging of the conformers since the SCS-MP2 energies were not available. These results were then compared with the experimental spectra.

Contrary to our expectations, all attempts to theoretically simulate the CD spectra of **3–5** turned out to be unsuccessful (Figure S-15 in Supporting Information). The exact reason remains to be elucidated, but possible reasons for this failure are as follows: (1) The dynamic behavior in solution was neglected in our calculation, but is actually more important.<sup>32</sup> Probably, the estimation of the conformer population by a simple Boltzmann approach was too simple. (2) We neglected vibrational Herzberg–Teller coupling effects in our calculations, but benzene’s <sup>1</sup>L<sub>b</sub> transitions are known in general to be strongly influenced by vibronic coupling.<sup>34</sup> (3) The current TD-DFT method with standard hybrid functionals is not accurate enough to describe the electronic through-space interactions (exciton coupling) in short distances. We recently reported that the theoretical CD spectra of some chiral cyclophanes were only

(27) Simaan, S.; Marks, V.; Gottlieb, H. E.; Stanger, A.; Biali, S. E. *J. Org. Chem.* **2003**, *68*, 637–640.

(28) Zavada, J.; Pankova, M.; Arnold, Z. *Coll. Czech. Chem. Commun.* **1976**, *41*, 1777–1790.

(29) (a) Seiders, T. J.; Baldrige, K. K.; Grube, G. H.; Siegel, J. K. *J. Am. Chem. Soc.* **2001**, *123*, 517–525. (b) Scott, L. T.; Hashemi, M. M.; Bratcher, M. S. *J. Am. Chem. Soc.* **1992**, *114*, 1920–1921. (c) Biederman, P. U.; Pogodin, S.; Agranat, I. *J. Org. Chem.* **1999**, *64*, 3655–3662.

(30) (a) Diedrich, C.; Grimme, S. *J. Phys. Chem. A* **2003**, *107*, 2524–2539. (b) Autschbach, J.; Ziegler, T.; van Gisbergen, S. J. A.; Baerends, E. *J. J. Chem. Phys.* **2002**, *116*, 6930–6940.

(31) For recent examples, see: (a) McCann, D. M.; Stephens, P. J. *J. Org. Chem.* **2006**, *71*, 6074–6098. (b) Stephens, P. J.; McCann, D. M.; Devlin, F. J.; Smith, A. B., III. *J. Nat. Prod.* **2006**, *69*, 1055–1064. (c) Gawronski, J. K.; Kwit, M.; Boyd, D. R.; Sharma, N. D.; Malone, J. F.; Drake, A. F. *J. Am. Chem. Soc.* **2005**, *127*, 4308–4319. (d) Schühly, W.; Crockett Sara, L.; Fabian Walter, M. F. *Chirality* **2005**, *17*, 250–6. (e) Forzato, C.; Furlan, G.; Nitti, P.; Pitacco, G.; Marchesan, D.; Coriani, S.; Valentin, E. *Tetrahedron: Asym.* **2005**, *16*, 3011–3023. (f) Zuber, G.; Goldsmith, M.-R.; Hopkins, T. D.; Beratan, D. N.; Wipf, P. *Org. Lett.* **2005**, *7*, 5269–5272. (g) Stephens, P. J.; McCann, D. M.; Cheeseman, J. R.; Frisch, M. J. *Chirality* **2005**, *17*, S52–S64.

(32) (a) Mori, T.; Inoue, Y.; Grimme, S. *J. Org. Chem.* **2006**, *71*, 9797–9806. See also: (b) Mori, T.; Ko, Y. H.; Kim, K.; Inoue, Y. *J. Org. Chem.* **2006**, *71*, 3232–3247. (c) Mori, T.; Inoue, Y. *Angew. Chem., Int. Ed.* **2005**, *44*, 2582–2585.

(33) For a recent treatment of the dynamic behavior on the simulation of the chiroptical properties, see: (a) Sebek, J.; Kejik, Z.; Bour, P. *J. Phys. Chem. A* **2006**, *110*, 4702–4711. (b) Glattli, A.; Daura, X.; Seebach, D.; van Gunsteren, W. F. *J. Am. Chem. Soc.* **2002**, *124*, 12972–12978. However, such treatment for the current system was practically unfeasible.

(34) (a) Vögtle, F.; Hünten, A.; Vogel, E.; Buschbeck, S.; Safarowsky, O.; Recker, J.; Parham, A.-H.; Knott, M.; Müller, W. M.; Müller, U.; Okamoto, Y.; Kubota, T.; Lindner, W.; Francotte, E.; Grimme, S. *Angew. Chem., Int. Ed.* **2001**, *40*, 2468–2471. (b) Parac, M.; Grimme, S. *Chem. Phys.* **2003**, *292*, 11–21.

TABLE 1. Computation Results for All Conformations of **2**<sup>a</sup>

	SCS-MP2 energy (Hartree)	$\Delta E$ (SCS-MP2) (kcal mol <sup>-1</sup> )	%population	%population ( <i>anti</i> only)	DFT-D energy (Hartree)	$\Delta E$ (DFT-D) (kcal mol <sup>-1</sup> )	%population	%population ( <i>anti</i> only)	specific rotation (aug-cc-pVDZ)	specific rotation (aug-SVP)
<b>2a</b>	-1699.2443	≅0	5.8	48.1	-1702.7025	≅0	3.4	39.7	1528	2339
<b>2b</b>	-1699.2441	+0.1	5.1	43.0	-1702.7024	+0.1	3.2	37.2	-2491	-2487
<b>2c</b>	-1699.2406	+2.3	0.6	4.9	-1702.7011	+0.9	1.5	16.8	-2715	-2653
<b>2d</b>	-1699.2403	+2.5	0.5	4.0	-1702.6995	+1.9	0.5	6.2	811	755
<b>2e</b>	-1699.2314	+8.1	0.0	0.0	-1702.6920	+6.6	0.0	0.1	2410	2339
<b>2f</b>	-1699.2311	+8.3	0.0	0.0	-1702.6922	+6.4	0.0	0.1	-3598	-3540
<b>2g</b>	-1699.2472	-1.9	37.0		-1702.7065	-2.5	42.8		-643	
<b>2h</b>	-1699.2474	-2.0	42.2		-1702.7061	-2.2	32.1		-2515	
<b>2i</b>	-1699.2450	-0.5	8.9		-1702.7050	-1.6	16.5		1637	
<b>2j</b>	-1699.2349	+5.9	0.0		-1702.6943	+5.1	0.0		-1039	
									-1205 (-437) <sup>b</sup>	(-44) <sup>b</sup>

<sup>a</sup> See Supporting Information for the structure of each conformer. <sup>b</sup> Averaged specific rotation for up-down/down-up conformers (**2a–f**).

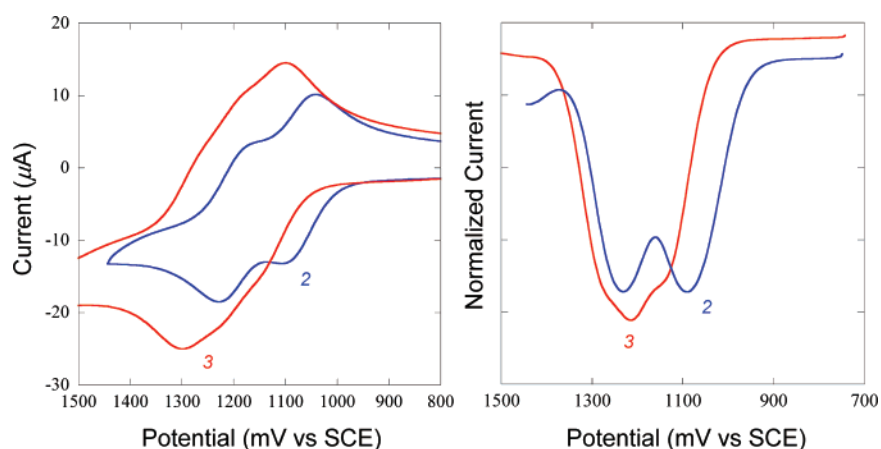


FIGURE 7. Comparison of cyclic voltammogram (left) and Osteryoung square-wave voltammogram (right) of **2** (blue) and **3** (red) in dichloromethane at a scan rate of 100 mV s<sup>-1</sup>.

reproduced by the more sophisticated CC2 method.<sup>35</sup> (4) The basic chromophores in **4** (distorted biphenylene) and **5** (geodesic corannulene) are not accurately described by the current density functionals.

#### (e) Theoretical and Experimental Optical Rotations of **2**.

The TD-DFT computations of optical rotations (OR) have become a routine tool in chiroptical studies and have been repeatedly employed for the prediction of absolute configuration.<sup>36</sup> We also performed the OR calculations for **2** with the BH-LYP functional using the aug-cc-pVDZ or aug-SVP basis-sets (Table 1). The calculated values for individual conformers were Boltzmann-averaged by using the most reliable single point SCS-MP2/TZVPP energies and compared with the experimental values. The calculated OR with the aug-cc-pVDZ basis-set are much larger (in absolute values) than the experimental values, and this was not improved even when the partially alternated (down-down) conformers were also taken into account. The calculated OR for each conformer showed reasonable agreement between the two basis-sets employed. However, the values obtained after averaging show large differences ( $-437^\circ$  versus  $-44^\circ$ ). Such a result can be attributed primarily to an incomplete cancelation of the dynamic effects between the conformers. We believe that the better results with the aug-SVP basis-set were

obtained incidentally, judging from the fact that the calculated specific rotations of **1** at the BH-LYP/aug-cc-pVDZ and aug-SVP levels are very similar to each other ( $-556^\circ$  and  $-555^\circ$ ), which are also ca. 13 times larger than the experimental value ( $-43^\circ$ ). The sign of the specific rotation was, nevertheless, always correctly predicted.

**Electrochemical Studies with **2** and **3**.** The cyclic voltammograms were obtained with dichloromethane solutions of **2** and **3** with tetra-*n*-butylammonium hexafluorophosphate as electrolyte (Figure 7, left). A stepwise and reversible oxidation–reduction curve was obtained for **2** at a scan rate of 100 mV s<sup>-1</sup>,  $E_{1/2}$  being determined to be 1.02 and 1.14 V vs SCE ( $\Delta E = 0.12$  V). Due to a larger solvation effect, considerably higher oxidation potentials (1.07 and 1.18 V) were found in a more polar solvent (acetonitrile). These values are in good agreement with those reported for the related achiral analogue ( $E_{1/2} = 1.07$  and 1.23 V vs SCE in dichloromethane).<sup>16</sup> Such an apparent stepwise oxidation of **2** with two identical donor arms indicates that there should be strong interaction between the arms in the ground state. The electrochemical behavior of the analogous *o*-xylylene-bridged donor is known to strongly depend on temperature, solvent, and sweep rate.<sup>16</sup> This was also the case with **2** (details of the effect of solvent and scan rate on the CV behavior are found in Figure S-16 in Supporting Information).

These results are in dramatic contrast to the CV behavior of **3**, where a quasi-single oxidation ( $3e$ ) at much higher potential was observed with all the scan rates examined (10–1000 mV s<sup>-1</sup>). The oxidation potential of **3** was determined to be 1.20 V

(35) (a) Muller, D. J.; Knight, A. E. W. *J. Phys. Chem.* **1984**, *88*, 3392–3395. (b) Berger, R.; Fischer, C.; Klessinger, M. *J. Phys. Chem. A* **1998**, *102*, 7157–7167.

(36) Mori, T.; Inoue, Y.; Grimme, S. *J. Phys. Chem. A* **2007**, *111*, 7995–8006.

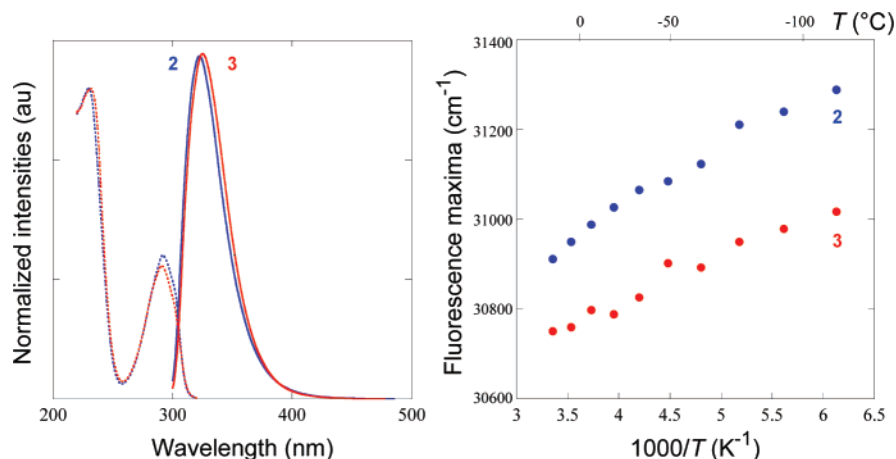


**FIGURE 8.** Left: Fluorescence spectra and fluorescence excitation spectra of **2** (0.01 mM, blue) and **3** (0.0067 mM, red) in methylcyclohexane at 25 °C. Excitation at 290 nm (dotted lines). Emission monitored at 320 nm (solid lines). Right: Arrhenius-type plots for the temperature dependence of the fluorescence maxima of **2** and **3** in methylcyclohexane.

vs SCE by a square-wave voltammogram (Figure 7, right), which is slightly larger than the  $E_{1/2}$  value reported for 2,6-dimethoxy-*p*-xylene and related molecules ( $\sim 1.0$  V), partially owing to the steric effect. It is to note that the peak was not completely single but that small shoulder peaks were also found, which indicates that appreciable, but relatively weak, interactions between the arms are operative in the oxidation process. A difference between the first and the second potentials,  $\Delta E = 0.09$  V, was evaluated from the Laplacian of the OSWV curve of **3**, which enabled us to estimate the stabilization energy of the radical cation by using the relationship:  $-RT \ln K = -\Delta EF$ , where  $F$  is the Faraday constant. Thus, the stabilization energy of radical cation **3**<sup>•+</sup> was calculated as 2.1 kcal mol<sup>-1</sup>, which is relatively smaller than the value for radical cation **2**<sup>•+</sup> (2.8 kcal mol<sup>-1</sup>). The stabilization energy of radical cation **3**<sup>•+</sup> is still significant in spite of the larger distance between the arms, compared with that in **2**<sup>•+</sup>. A large peak shift found between the oxidation and reduction cycle (0.19 V at a scan rate of 100 mV s<sup>-1</sup>) also supports the interaction between the arms of **3** in the oxidation process.

**Chemical Oxidation and the CD Spectral Changes of 2 and 3.** The Meerwein salt [Et<sub>3</sub>O<sup>+</sup>SbCl<sub>6</sub><sup>-</sup>] is known as an effective reagent particularly for the preparation of the cation radical salts with various aromatic aryl ethers with oxidation potentials lower than 1.5 V vs SCE. By using this oxidant, one can avoid the concomitant formation of byproduct(s),<sup>37</sup> allowing the formation of suitable crystals of pure paramagnetic aromatic cation radicals for X-ray structure determination. Upon mixing 1.5 equiv of Et<sub>3</sub>O<sup>+</sup>SbCl<sub>6</sub><sup>-</sup> into dichloromethane solutions of **2**

or **3** under argon atmosphere, new absorption bands gradually developed at 400–500 nm, which are assignable to a dialkoxy-*p*-xylyl radical cation (Figure S-17, left, in Supporting Information). The CD spectra of the same solutions were also measured after oxidation for 10 h (Figure S-17, right). Relatively weak positive Cotton effects were observed at this absorption band among the drifting spectra. We did not further study the CD spectral changes upon chemical oxidation, since, unfortunately, the spectra did not appear to provide insights into the conformational changes upon oxidation. Such a weak Cotton effect observed at the D-D transition seems to be a common feature of radical cations.<sup>38</sup>

**Excited-State Properties of 2 and 3.** The steady-state fluorescence spectra of **2** and **3** were recorded in methylcyclohexane at varying temperatures (Figure 8). The fluorescence quantum yields of both **2** and **3** were determined as 0.27 at 25 °C, which are comparable to that of the parent 2,5-dimethoxy-*p*-xylene ( $\phi_{\text{FL}} = 0.30$ ).<sup>39</sup> No exciplex or excimer emission was observed upon excitation of **2** under the experimental conditions examined. A small red-shift in the fluorescence emission observed for **3**, relative to that of **2**, can be ascribed to the larger stabilization by the through-bond electronic resonance with the additional aromatic side-arm in the excited-state of **3**. Fluorescence maxima were gradually shifted to the blue as the temperature of the solution decreased. This suggests that there exists quite large stabilization by reorientation of the arms in their excited states, and such a conformational change requires some activation energy. This assumption is in accord with the fact that there is a dynamic conformational alteration process of the chiral side-arms in solution in the ground state (*vide supra*) and in the excited-state as well. Thus, the plots of the fluorescence maxima (in energy unit) against the reciprocal temperature afforded good straight lines for both compounds. The temperature dependence was found more pronounced for **2** than for **3**, probably because of the larger stabilization in the

(37) For recent examples, see: (a) Mort, B. C.; Autschbach, J. *J. Phys. Chem. A* **2006**, *110*, 11381–11383. (b) Kundrat, M. D.; Autschbach, J. *J. Phys. Chem. A* **2006**, *110*, 4115–4123. (c) Autschbach, J.; Jensen, L.; Schatz, G. C.; Tse, Y. C. E.; Krykunov, M. *J. Phys. Chem. A* **2006**, *110*, 2461–2473. (d) Durandin, A.; Jia, L.; Crean, C.; Kolbanovskiy, A.; Ding, S.; Shafirovich, V.; Broyde, S.; Geacintov, N. E. *Chem. Res. Toxicol.* **2006**, *19*, 908–913. (e) Giorgio, E.; Roje, M.; Tanaka, K.; Hamersak, Z.; Sunjic, V.; Nakanishi, K.; Rosini, C.; Berova, N. *J. Org. Chem.* **2005**, *70*, 6557–6563. (f) Crawford, T. D.; Owens, L. S.; Tam, M. C.; Schreiner, P. R.; Koch, H. *J. Am. Chem. Soc.* **2005**, *127*, 1368–1369. (g) Grimme, S.; Furche, F.; Ahlrichs, R. *Chem. Phys. Lett.* **2002**, *361*, 321–328. (h) Grimme, S. *Chem. Phys. Lett.* **2001**, *339*, 380–388. (i) Ruud, K.; Helgaker, T. *Chem. Phys. Lett.* **2002**, *352*, 533–539. (j) Autschbach, J.; Patchkovskii, S.; Ziegler, T.; van Gisbergen, S. J. A.; Baerends, E. J. *J. Chem. Phys.* **2002**, *117*, 581–592. (k) Stephens, P. J.; Devlin, F. J.; Cheeseman, J. R.; Frisch, M. J. *J. Phys. Chem. A* **2001**, *105*, 5356–5379.

(38) (a) Rathore, R.; Burns, C. L.; Deselnicu, M. I.; Denmark, S. E.; Bui, T. *Org. Synth.* **2005**, *82*, 1–9. (b) Rathore, R.; Kumar, A. S.; Lindeman, S. V.; Kochi, J. K. *J. Org. Chem.* **1998**, *63*, 5847–5856.

(39) (a) Mori, T.; Ko, Y. H.; Kim, K.; Inoue, Y. *J. Org. Chem.* **2006**, *71*, 3232–3247. (b) Mori, T.; Inoue, Y. *Angew. Chem., Int. Ed.* **2005**, *44*, 2582–2585. (c) Mori, T.; Inoue, Y. *J. Phys. Chem. A* **2005**, *109*, 2728–2740. (d) Mori, T.; Izumi, H.; Inoue, Y. *J. Phys. Chem. A* **2004**, *108*, 9540–9549.

excited-state of **2**, owing to the chiral side-arms placed in the ortho position. By the Arrhenius-type treatment, the activation energies were evaluated as  $E_a = 27.0 \text{ kcal mol}^{-1}$  for **2** and  $20.2 \text{ kcal mol}^{-1}$  for **3**, respectively. These values are much larger than the energy for the rotation of small ethyl group (barrier of conformational alteration:  $9\text{--}12 \text{ kcal mol}^{-1}$ ) in the polyethylenes,<sup>20,40</sup> but still in an energy range accessible at ambient temperatures.

## Summary and Conclusions

We prepared new multiarmed chiral aryl ethers (**2–5**) containing two, three, five, or eight side-arms on a series of gradually expanded aromatic cores and investigated the conformation and dynamic behavior of the side-arms to find that the CD spectra measured at varying temperatures are very informative. While the fully side-arm-alternated conformers are most stable in **2** and **3**, the syn-conformer of **2** or the partially alternated conformer **3** is also important in solution to interpret all the spectroscopic observations. Scheme 1 illustrates the conformational variations of **2–5**. Important findings are summarized as follows:

(1) X-ray crystallographic analyses: Two anti-conformers (up–down and down–up) were found in a 1:1 ratio in crystalline **2**. The crystal structure of **3** shows that the fully alternated up-down disposition is favored. Thus, all the chiral side-arms in **3** are syn with respect to the central ring in the solid state.

(2) DFT-D calculations: dispersion-corrected DFT calculations at the B-LYP/TZVP level yielded six anti- and four syn-conformers of **2**, only two each of which were found to be important. The geometries of the two calculated anti-conformers are in good agreement with the X-ray structures. The calculations with the same level of theory afforded the syn-**3**, fully alternated **4**, as well as  $C_5$ -symmetric **5** as the stable conformers.

(3) <sup>1</sup>H NMR and UV–vis spectra: These spectra of poly-tentacled donors were investigated in detail at different temperatures to afford important information about the conformation of the molecules (gradual freezing of the side-arms upon cooling), although the fast isomerization of the side-arms to form partially alternated conformers (side-arm alteration) could not be tracked.

(4) Temperature dependence of the CD spectra: In contrast, the low-temperature CD spectra of **2** and **3** provided important insights into such behavior. By decreasing the temperature, an increased negative Cotton effect at the <sup>1</sup>L<sub>b</sub> band was only evident for compounds **1**, **4**, and **5**. Because of the attractive van der Waals interactions between the arms in nonpolar solvents, the syn-conformations become increasingly significant for **2** at low temperatures to induce a weak positive Cotton effect at the <sup>1</sup>L<sub>b</sub> band. A much larger positive Cotton effect was observed for **3** at the <sup>1</sup>L<sub>b</sub> band due to the  $C_3$ -symmetric conformer. A rapid increase of this positive Cotton effect with decreasing temperature can be explained by a larger population of partially alternated conformers and/or slower alteration of the side-arms at the low temperatures.

(5) Electrochemistry and fluorescence spectra: While a stepwise and reversible oxidation–reduction (1.02 and 1.14 V vs SCE) was found in the CV of **2**, a quasi-single oxidation at much higher potential (1.20 V) was observed for **3**. The

stabilization energy of radical cation of **2** ( $2.8 \text{ kcal mol}^{-1}$ ) was found larger than that of **3** ( $2.1 \text{ kcal mol}^{-1}$ ). Both **2** and **3** exhibited strong fluorescence upon electronic excitation ( $\phi_{\text{FL}} = 0.27$ ). By Arrhenius plots of the fluorescence maxima, the activation energies of side-arm alteration were evaluated as  $E_a = 27.0 \text{ kcal mol}^{-1}$  and  $20.2 \text{ kcal mol}^{-1}$ , for **2** and **3**, respectively.

By using a chiral probe and experimental and theoretical CD spectra, the dynamic behavior of the side-arms of the multiarmed aryl ethers in solution was revealed for the first time. Thus, the syn-conformation in bipodal donors and the partially alternated conformation in 1,3,5-tripodal donors turned out to be more important in solution, than were previously thought, in interpreting the given spectroscopic features. The investigation of X-ray structures alone is therefore not sufficient to understand the conformations of multiply substituted host molecules in condensed phase.

## Experimental Section

**Preparation of Multiarmed Chiral Donors.** The chiral ether **1** was prepared by Mitsunobu reaction<sup>41</sup> of 2-methyl-4-methoxyphenol with (*S*)-2-butanol. Compounds **2–4**, which contain two, three, or eight chiral donor tether groups, were prepared by Ag<sup>+</sup>-promoted aryl substitution of the corresponding benzyl bromides.<sup>27</sup> The chiral corannulene derivative **5**, which bears somewhat different chiral aromatic side-arms with the same (*R*)-2-methylpropyloxy group, was prepared by Ni-catalyzed arylation of *sym*-pentachlorocorannulene.<sup>42</sup> A range of core molecules (benzene, biphenylene, and corannulene) were selected in this study in order to investigate the effect of different scaffolds on the conformational and dynamic behavior of the side-arms in solution. The same chiral donor (similar one in the case of **5**) was selected as side-arm, which enabled us to study the conformational behavior in solution by experimental (and some theoretical) circular dichroism. Details of the synthetic procedure and full characterization details are described below or found in the Supporting Information.

**1,2-Bis(2-methoxy-4-methyl-5-(*R*)-2-methylpropyloxytolyl)tetramethylbenzene (2).** Yield: 16%. Mp: 115–116 °C (diethyl ether/ethanol). <sup>1</sup>H NMR: 0.81 (6H, t,  $J = 7.6 \text{ Hz}$ ), 1.07 (6H, d,  $J = 6.4 \text{ Hz}$ ), 1.41 (2H, pseudo sept,  $J = 7.6 \text{ Hz}$ ), 1.57 (2H, pseudo sept,  $J = 7.6 \text{ Hz}$ ), 2.08 (6H, s), 2.17 (6H, s), 2.25 (6H, s), 3.75 (6H, s), 3.77 (2H, m,  $J = 5.6 \text{ Hz}$ , peaks are overlapped), 3.79 (4H, s), 6.12 (2H, s), and 6.61 (2H, s). <sup>13</sup>C NMR: 9.7, 16.4, 16.8, 17.0, 19.4, 29.1, 29.8, 56.0, 76.2, 112.9, 116.3, 125.6, 127.4, 133.08, 133.12, 134.6, 149.9, and 151.2. MS (EI, direct):  $m/z = 547$  ( $M^+ + 1$ , 29%), 546 ( $M^+$ , 100), 339 (16), 321 (14), 295 (25), 284 (12), 283 (27), 279 (24), 266 (18), 265 (49), 250 (19), 207 (13), 151 (42), 147 (38), 125 (26), and 121 (17). HRMS (EI): 546.3707.  $C_{36}H_{50}O_4$  requires 546.3709. EA: Found: C, 78.82; H, 9.25%. Calcd for  $C_{36}H_{50}O_4$ : C, 79.08; H, 9.22; O, 11.70. Specific rotation:  $[\alpha]_D^{25} -21.9 \pm 4.2^\circ$  ( $c$  0.10,  $CHCl_3$ ).

**1,3,5-Tris(2-methoxy-4-methyl-5-(*R*)-2-methylpropyloxytolyl)triethylbenzene (3).** Yield: 20%. Mp: 105–106 °C (dichloromethane/ethanol). <sup>1</sup>H NMR: 0.65 (9H, t,  $J = 7.6 \text{ Hz}$ ), 0.95 (9H, d,  $J = 6.0 \text{ Hz}$ ), 1.09 (9H, t,  $J = 7.6 \text{ Hz}$ ), 1.22–1.45 (6H, m,  $J = 7.2 \text{ Hz}$ ), 2.15 (9H, s), 2.46 (6H, q,  $J = 7.2 \text{ Hz}$ ), 3.62 (3H, sxt,  $J = 6.0 \text{ Hz}$ ), 2.84 (9H, s), 3.92 (3H, t,  $J = 18.0 \text{ Hz}$ ), 4.06 (3H, t,  $J = 18.0 \text{ Hz}$ ), 6.09 (3H, s), and 6.64 (3H, s). <sup>13</sup>C NMR: 9.2, 15.6, 16.4, 19.3, 23.7, 28.1, 28.5, 56.2, 76.1, 113.1, 116.6, 125.9, 127.5, 141.3, 150.1, and 151.0. MS (EI, direct):  $m/z = 781$  ( $M^+ + 1$ , 17%), 780

(41) (a) Marks, V.; Gottlieb, H. E.; Biali, S. E. *J. Am. Chem. Soc.* **1997**, *119*, 9672–9679. (b) Taha, M.; Marks, V.; Gottlieb, H. E.; Biali, S. E. *J. Org. Chem.* **2000**, *65*, 8621–8628. (c) Marks, V.; Gottlieb, H. E.; Melman, A.; Byk, G.; Cohen, S.; Biali, S. E. *J. Org. Chem.* **2001**, *66*, 6711–6718.

(42) (a) Mitsunobu, O. *Synthesis* **1981**, 1–28. (b) Huges, D. L. *Org. Prep. Proced. Int.* **1996**, *28*, 127–164. (c) Dodge, J. A.; Jones, S. A. *Rec. Res. Dev. Org. Chem.* **1997**, *1*, 273–283.

(40) Mori, T.; Takamoto, M.; Wada, T.; Inoue, Y. *Helv. Chim. Acta* **2001**, *84*, 2693–2707.

(M<sup>+</sup>, 33%), 612 (19), 306 (16), 207 (23), 152 (10), 151 (100), and 121 (10). HRMS (EI): 780.5337. C<sub>51</sub>H<sub>72</sub>O<sub>6</sub> requires 780.5329. EA: Found: C, 78.23; H, 9.30%. Calcd for C<sub>51</sub>H<sub>72</sub>O<sub>6</sub>: C, 78.42; O, 12.29; H, 9.29. Specific rotation:  $[\alpha]^{25}_{\text{D}} -25.2 \pm 5.8^{\circ}$  (*c* 0.10, CHCl<sub>3</sub>).

**Octakis(2-methoxy-4-methyl-5-(*R*)-2-methylpropyloxytolyl)-biphenylene (4).** Yield: 3%. <sup>1</sup>H NMR: 0.90 (24H, t, *J* = 7.6 Hz), 1.17 (6H, d, *J* = 6.0 Hz), 1.49 (8H, pseudo sept, *J* = 7.6 Hz), 1.63 (8H, pseudo sept, *J* = 7.8 Hz), 2.04 (24H, s), 2.19 (16H, s), 3.74 (24H, s), 3.96 (8H, sxt, *J* = 6.0 Hz), 6.40 (8H, s), and 6.62 (8H, s). <sup>13</sup>C NMR: 9.8, 16.4, 16.5, 19.5, 29.2, 55.9, 76.2, 113.0, 115.7, 124.8, 125.9, 126.62, 137.8, 147.9, 145.0, and 151.2. MS (FD): *m/z* = 1802.16 (M<sup>+</sup> + 1). MS (FAB): *m/z* = 1802.17 (M<sup>+</sup> + 1). C<sub>116</sub>H<sub>152</sub>O<sub>16</sub> requires 1801.11. Specific rotation:  $[\alpha]^{25}_{\text{D}} -15.6 \pm 4.1^{\circ}$  (*c* 0.10, CHCl<sub>3</sub>).

**1,3,5,7,9-Pentakis[*p*-(*R*)-methylpropyloxyphenyl]coranulene (5).** Yield: 45%. <sup>1</sup>H NMR: 1.03 (15H, t, *J* = 7.5 Hz), 1.36 (15H, d, *J* = 6.0 Hz), 1.68 (5H, pseudo sept, *J* = 7.5 Hz), 1.82 (5H, pseudo sept, *J* = 7.5 Hz), 4.38 (5H, pseudo sxt, *J* = 6.0 Hz), 6.97 (10H, d, *J* = 8.6 Hz), 7.54 (10H, d, *J* = 8.6 Hz), and 7.76 (5H, s). <sup>13</sup>C NMR: 10.0, 19.5, 29.4, 75.2, 116.0, 125.3, 129.4, 131.3, 132.2, 135.3, 141.8, and 158.2. HRMS (FAB): 990.5231. C<sub>70</sub>H<sub>70</sub>O<sub>5</sub> requires 990.5223. EA: Found: C, 84.58; H, 7.08%. Calcd for C<sub>70</sub>H<sub>70</sub>O<sub>5</sub>: C, 84.81; H, 7.12; O, 8.07. Specific rotation:  $[\alpha]^{25}_{\text{D}} -45.8 \pm 4.5^{\circ}$  (*c* 0.10, CHCl<sub>3</sub>).

#### Technical Details of the Quantum Chemical Computations.

All calculations were performed on Linux-PCs using the TURBOMOLE 5.8 program suite.<sup>43</sup> All conformers were fully optimized at the dispersion-corrected DFT-D-B-LYP level<sup>44</sup> employing C<sub>2</sub>, C<sub>3</sub>, or C<sub>5</sub> symmetry constraint, where appropriate, by using an AO basis set of valence triple- $\zeta$  quality with a set of polarization functions (denoted as TZVP;<sup>45</sup> in standard notation: H, [3s1p], C/O, [5s3p1d]), and numerical quadrature grid m4. The most stable Tg<sup>-</sup> conformation was employed for the chiral alkyl group throughout this study.<sup>26</sup> This conformation was found also in the X-ray crystal structures of **2** and **3** in this study (*vide infra*). The resolution of identity (RI) approximation<sup>47</sup> was employed in all DFT-D-B-LYP calculations, and the corresponding auxiliary basis sets were taken from the TURBOMOLE basis-set library. Subsequent single-point energy calculations were performed with the spin-component-scaled (SCS)-MP2 method<sup>22</sup> with a TZVPP basis-set that has additional d/f and p/d functions on non-hydrogen and hydrogen atoms, respectively. It has been shown that this simple modification of the standard MP2 scheme, termed SCS-MP2, leads to dramatic improvements in accuracy of calculated energies, particularly for molecules with weak interactions where standard DFT fails.<sup>48</sup> The method is expected to provide the most accurate relative energies (comparable to the computationally highly demanding CCSD(T)

calculations) and was thus used to obtain the final Boltzmann distribution at 298 K of the conformers. Details are reported in Supporting Information.

All excited-state calculations have been performed at the optimized ground-state geometries and thus correspond to vertical transitions. The CD (and UV-vis) spectra of **1** and **2** were simulated on the basis of time-dependent density functional theory (TD-DFT)<sup>29</sup> with the BH-LYP<sup>49</sup> functional and employing the TZVP basis set. The program module escf<sup>50</sup> has been used in these TD-DFT treatments. The CD spectra were simulated by overlapping Gaussian functions for each transition where the width of the band at 1/*e* height is fixed at 0.4 eV and the resulting intensities of the combined spectra were scaled to the experimental values. As usual, the calculated band intensities are larger than their experimental counterparts and are thus scaled to facilitate comparison with experiment. The somewhat smaller scaling factors found (1/5 and 1/20, for **1** and **2**, respectively, in contrast to standard 1/2–1/3) are probably due to our ignorance of the dynamic behavior in the present theoretical treatments (see also ref 26 for more discussion). Because of a systematic overestimation of the transition energies compared to the experiment in the BH-LYP calculations, the spectra were uniformly shifted by 0.5 eV. The optical rotations at the sodium-D line wavelength of **1** and **2** were also calculated at the TD-DFT-BH-LYP method using Dunning's aug-cc-pVDZ<sup>51</sup> and the aug-SVP<sup>52</sup> basis-sets (H, [3s2p], C/O, [4s3p2d]). The rotational strengths from the length-gauge representation, which are known to be numerically more robust, were used throughout. It is known that in the absence of GIAOs, these values are origin-dependent. Strictly speaking, the calculated optical rotations and CD intensities can only be compared to experimental values when they are origin-independent, but the length and velocity rotational strengths converge to the same value in the complete basis-set limit. With our relatively large triple- $\zeta$  type AO basis-sets, the differences between both representations were negligible (differences are mostly less than 2–3%).

**Acknowledgment.** T.M. thanks the Alexander von Humboldt-Stiftung for the fellowship. We thank Drs. Christian Mück-Lichtenfeld, Christian Diedrich, and Manuel Piacenza for technical assistance and fruitful discussion of the theoretical data. Financial support of this work by a Grant-in-Aid for Scientific Research from the Ministry of Education, Culture, Sports, Science, and Technology of Japan to T.M. is gratefully acknowledged.

**Supporting Information Available:** Details of experimental procedure and computation, X-ray crystallographic structure determination (CCDC 650013 and 650014) as well as CIF files of **2** and **3**, cyclic voltammometric studies of **1** and **3**, <sup>1</sup>H and <sup>13</sup>C NMR charts and theoretical and experimental UV-vis and CD spectra of **1–5** under a variety of conditions, and Cartesian coordinates of the optimized geometries of a variety of conformations of **1–5**. This material is available free of charge via the Internet at <http://pubs.acs.org>.

JO071216N

(43) Grube, G. H.; Elliott, E. L.; Steffens, R. J.; Jones, C. S.; Baldrige, K. K.; Siegel, J. S. *Org. Lett.* **2003**, *5*, 713–716.

(44) Ahlrichs, R.; Bär, M.; Baron, H.-P.; Bauernschmitt, R.; Böcker, S.; Crawford, N.; Deglmann, P.; Ehrig, M.; Eichkorn, K.; Elliott, S.; Furche, F.; Haase, F.; Häser, M.; Horn, H.; Hättig, C.; Huber, C.; Huniar, U.; Kattannek, M.; Köhn, A.; Kölmel, C.; Kollwitz, M.; May, K.; Nava, P.; Ochsenfeld, C.; Öhm, H.; Patzelt, H.; Rappoport, H. D.; Rubner, O.; Schäfer, A.; Schneider, U.; Sierka, M.; Treutler, O.; Unterreiner, B.; von Arnim, M.; Weigend, F.; Weis, P.; Weiss, H. *TURBOMOLE version 5.8*; Universität Karlsruhe: Karlsruhe, 2005. See also: [http://www.cosmologic.de/QuantumChemistry/main\\_turbomole.html](http://www.cosmologic.de/QuantumChemistry/main_turbomole.html).

(45) Grimme, S. *J. Comput. Chem.* **2004**, *25*, 1463–1473.

(46) Schäfer, A.; Huber, C.; Ahlrichs, R. *J. Chem. Phys.* **1994**, *100*, 5829–5835.

(47) (a) Eichkorn, K.; Treutler, O.; Öhm, H.; Häser, M.; Ahlrichs, R. *Chem. Phys. Lett.* **1995**, *240*, 283–289. (b) Weigend, F.; Häser, M. *Theor. Chem. Acc.* **1997**, *97*, 331–340. (c) Grimme, S.; Waletzke, M. *Phys. Chem. Chem. Phys.* **2000**, *2*, 2075–2081. (d) Vahtras, O.; Ahlrichs, R.; Feyereisen, M. W. *Chem. Phys. Lett.* **1993**, *213*, 514–518. (e) Hättig, C.; Weigend, F. *J. Chem. Phys.* **2000**, *113*, 5154–5161.

(48) (a) Grimme, S. *Angew. Chem., Int. Ed.* **2006**, *45*, 4460–4464, and references cited therein. (b) Grimme, S.; C. Diedrich, S.; Korth, M. *Angew. Chem., Int. Ed.* **2006**, *45*, 625–629.

(49) Notations from Gaussian package corresponds to BH&HLYP. See also: (a) Maity, D. K.; Duncan, W. T.; Truong, T. N. *J. Phys. Chem. A* **1999**, *103*, 2152–2159. (b) Duncan, W. T.; Truong, T. N. *J. Chem. Phys.* **1995**, *103*, 9642–9652. (c) Liao, M.-S.; Lu, Y.; Scheiner, S. *J. Comput. Chem.* **2003**, *24*, 623–631.

(50) Bauernschmidt, R.; Ahlrichs, R. *Chem. Phys. Lett.* **1996**, *256*, 454–464.

(51) Dunning, T. H. *J. Chem. Phys.* **1993**, *98*, 7059–7071. (b) Kendall, R. A.; Dunning, T. H.; Harrison, R. J. *J. Chem. Phys.* **1992**, *96*, 6796–6806.

(52) Hobza, P.; Sponer, J. *J. Am. Chem. Soc.* **2002**, *124*, 11802–11808.